American Mineralogist, Volume 64, pages 1312-1321, 1979

Determination of liquid compositions in high-pressure melting of peridotite

A. L. JAQUES[1] AND D. H. GREEN

Department of Geology, University of Tasmania
Hobart, Tasmania 7001

Abstract

Experimental problems in the determination of liquid compositions from the partial melting of peridotite are examined in the light of data obtained in an experimental study of the anhydrous melting of peridotite. A scanning electron microscope coupled with an energy-dispersive microprobe has been employed to examine the nature of quench phases and their effect on the melt composition, and to examine the effect of iron loss on crystal–melt equilibria. In most cases the problems of iron loss, non-equilibrium, and quench modification of the melt composition preclude direct determination of the composition of partial melts, even under anhydrous conditions. Provided the modal proportions and compositions of residual phases are known, and due allowance made for preferential adjustment of residual phases to iron loss, the compositions of equilibrium partial melts may be obtained by mass-balance calculations.

Introduction

It is now generally recognized that basaltic magmas arise by partial melting of upper mantle peridotite, dominated by magnesian olivine and orthopyroxene. Accurate determination of the liquid compositions formed by partial melting of peridotite under known conditions (melt proportion, temperature, pressure, residual phase compositions and proportions, and volatile content) is therefore an important goal in experimental petrology. A number of studies towards this end have been attempted on a variety of natural peridotite compositions under differing P–T conditions and volatile contents.

In the earliest studies, phase relations only were determined and liquid compositions broadly inferred (*e.g.* Ito and Kennedy, 1967). In later experiments the compositions of the residual crystals and the quenched glass were determined by electron microprobe and the percentage of melt estimated visually (*e.g.* Kushiro *et al.*, 1972; Mysen and Boettcher, 1975; Nehru and Wyllie, 1975). More recently Mysen and Kushiro (1977) have used beta-track counting of charges spiked with radioactive tracers to more accurately determine the percentage of melting and have relied on microprobe analysis of quenched glasses to yield compositions of the melt phase.

Implicit in this experimental approach is the assumption that the directly determined quenched glass composition is that of the equilibrium melt for those particular conditions. This assumption can be criticized on two grounds. Firstly, iron loss from the sample to the noble-metal capsules used in partial melting experiments is well documented (*e.g.*, Nehru and Wyllie, 1975; Green, 1976; and others). The extent of iron loss is dependent on temperature and run duration, and since iron is not lost uniformly from the charge, Fe/Mg partitioning between crystal and liquid varies as a function of run duration (Stern and Wyllie, 1975; see below). Apart from changing the MgO/FeO ratio of the silicate charge, iron loss also increases the silica saturation of the bulk composition and probably of any melt component (O'Hara and Humphreys, 1977). Secondly, the growth of metastable quench crystals during the quenching of the glass can significantly modify the composition of the glass from that of the equilibrium melt (Green, 1973, 1976; Cawthorn *et al.*, 1973; Nicholls, 1974). These problems in the direct determination of the equilibrium partial melt composition have been the focus of debate in the past concerning the hydrous melting of peridotite (*e.g.* Mysen *et al.*, 1974; Green, 1973, 1976). Green showed that these problems could be

[1] Present address: Bureau of Mineral Resources, Canberra City, A.C.T. 2601, Australia.

0003–004X/79/1112–1312$02.00

overcome and a reliable estimate of the equilibrium melt could be calculated from a knowledge of the composition of the residual phases and the bulk charge using crystal/liquid partition data.

Mysen and Kushiro (1977) considered that these problems did not greatly effect the results of their study on the anhydrous melting of peridotite, and presented a suite of glass compositions ranging from 'alkali picrite' to 'olivine tholeiite' to 'peridotitic komatiite' as the equilibrium melts from peridotite. While the compositional range of liquids is consistent with earlier interpretations of melting at this pressure (Green and Ringwood, 1967) and is broadly that anticipated over such a melting interval, discrepancies among the data cast doubt on the validity of these directly determined glass compositions as the true unmodified equilibrium melts for the stated percentage of melting. As part of a similar melting study we have evaluated the problems involved in conducting such experiments, and find that the problems can be severe enough in many cases to preclude direct determination of equilibrium melt compositions. Here we present an alternative approach for calculation of equilibrium liquid compositions.

Experimental methods

Technique

Two peridotite compositions derived from pyrolite (Ringwood, 1966; Green, 1973, 1976) and Tinaquillo peridotite (Green, 1963) have been studied. In each case the composition used in the experiments is that of the peridotite minus 40 percent olivine to facilitate identification of minor phases and increase the relative proportion of melt and minor phases without eliminating olivine. Compositions (Table 1) were prepared from AR grade chemicals and sintered at 1000°C.

Experiments were carried out in a solid-media (piston cylinder) high-pressure apparatus, using piston-in technique and a pressure correction of minus 10 percent nominal piston pressure. Temperatures were measured by a Pt–Pt90Rh10 thermocouple with no correction for the effect of pressure on the thermocouple emf. Pyrex-glass sleeves with graphite inserts were used in 0.5-inch diameter furnace assemblies to minimize hydrogen diffusion from the dehydrating outer talc sleeve. Samples (15–20 mg) were sealed in Pt capsules and preheated at 900°–1000°C for 8–12 hours, packed in metallic iron powder in an attempt to presaturate the capsule in iron. All runs were anhydrous and the powdered starting mix was dried overnight at 110°C. Spec-pure iron capsules were used in some short-duration runs. These experiments produced an fO_2 lower than that in the Pt capsules, resulting in elimination of chrome spinel, and in some cases the charge dissolved iron from the capsule.

Table 1. Compositions of starting material

	Pyrolite - 40% olivine	Tinaquillo peridotite - 40% olivine
SiO_2	47.9	47.5
TiO_2	1.18	0.13
Al_2O_3	5.91	5.35
Fe_2O_3	0.20	0.15
FeO	8.63	7.38
MnO	0.13	0.18
MgO	28.8	32.8
CaO	5.14	4.99
Na_2O	0.95	0.30
K_2O	0.22	0.03
P_2O_5	-	0.02
Cr_2O_3	0.72	0.75
NiO	0.18	0.43
$100Mg/Mg+Fe^{++}$	85.6	88.8
100Mg/Mg+ Fe	85.3	88.6

Microprobe analysis

The charge was recovered as a coherent cylinder of crystals and glass. A portion of one split was examined in refractive-index oils. The polished mount containing the other split was examined optically in reflected light and by scanning electron microscope using a JEOL JX 50A electron microprobe–scanning electron microscope (SEM) fitted with an energy-dispersive (EDAX) analytical system. Simultaneous quantitative analysis for 10 elements (Na to Fe) of residual phases, quench phases, glass, and bulk charge was obtained by the method of Reed and Ware (1973, 1975). Optimization of the backscattered and secondary electron images enabled clear resolution and discrimination of all phases including melt and quench crystals at up to 2000 times magnification (Fig. 1). Discrimination of phases was based on both form and contrast from the back-scattered electron image, which is dependent on the mean atomic number of the target. In this way Fe-rich rims on primary phases and quench phases, *e.g.* quench clinopyroxene, can be distinguished by the higher Fe, Al, and Ti contents compared to the primary equilibrium phases. Glass analyses and analyses of the bulk charge were made with rapid reduced-area scans to

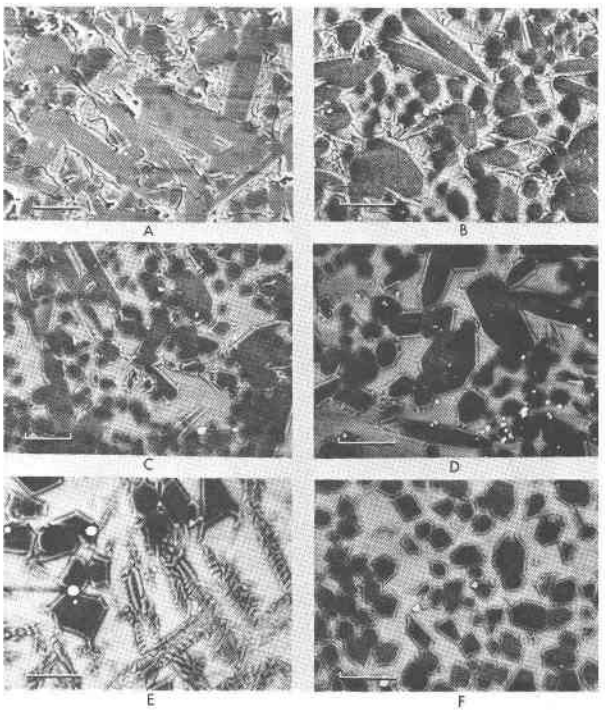

Fig. 1. Scanning electron microscope photographs of partial melting runs of pyrolite − 40 percent olivine and spinel lherzolite − 40 percent olivine, showing metastable quench phases. Scale bar is 20μ long. Quench outgrowths of clinopyroxene appear bright, as do thin quench rims of more Fe-rich olivine on primary olivine (note Figs. 1E, F particularly). (A) Pyrolite, 15 kbar, 1350°C. A low percentage melting run. Residual phases are olivine (small dark euhedra), orthopyroxene (large tabular crystals), clinopyroxene (small lighter euhedra), and chrome spinel (tiny bright euhedra). Melt is light interstitial material. Quench clinopyroxene forms light-colored rims on residual phases. Note the drastic reduction of the liquid volume by the quench phases. Compositions of phases are given in Table 4. (B) Pyrolite, 15 kbar, 1400°C. Quench clinopyroxene forms rims on residual olivine and orthopyroxene. Note the presence of some discrete quench clinopyroxene in the glass (crosses, lower right) and the larger percentage of melt. (C) Pyrolite, 10 kbar, 1300°C. Quench clinopyroxene rims residual olivine and orthopyroxene, and forms discrete crystals in the glass (small crosses, lower center). Compositions given in Table 3. (D) Pyrolite, 10 kbar, 1350°C. Like C but note the higher percentage of melt. Quench clinopyroxene is less abundant and modification of the glass composition is less severe than for A, B, and C. (E) Pyrolite, 10 kbar, 1450°C. Skeletal and dendritic quench low-calcium pyroxene forming conical spirals in glass, and dendritic rims on residual olivine. Note the similarity in the quench forms to those found in some komatiites. (F) Spinel lherzolite, 10 kbar, 1450°C. Quench low-calcium pyroxene and olivine on residual olivine. Compositions given in Table 5.

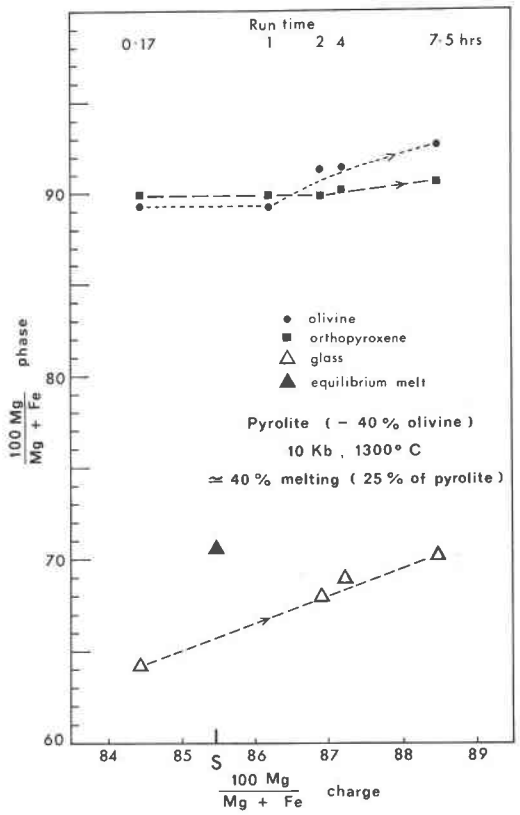

Fig. 2. 100Mg/(Mg+Fe) ratios of the residual phase (excluding Cr spinel) and glass with varying run times. S = starting composition. Olivine and glass compositions become increasingly Mg-rich as iron is lost from the charge with increasing run time. The capsules used in the 2-, 4-, and 7½-hour runs were packed in metallic iron powder for 8–12 hours at 900–1000°C in an attempt to presaturate the capsule in iron. Compositional data from Table 3.

minimize alkali volatilization and ensure representative analysis. The ability of scanning electron microscopy to discriminate phases such as olivine and orthopyroxene, clinopyroxene and glass, and to reveal compositional differences (quench rims) within phases is demonstrated in Figure 1 and confirmed by quantitative analyses of the visually discriminated areas. This technique thus permits modal analysis of these fine-grained experimental charges.

Modal analysis

Modal analysis, including the percentage of melt, was made by point counting of the SEM photographs using a 10 cm × 9 cm transparent grid; all quench phases were counted as glass. A minimum of 1200 points were counted in replicate and averaged.

Calculation of equilibrium liquid compositions

The compositions of the equilibrium liquids were calculated by mass balance after conversion of the volume percent modes to weight percent modes from appropriate mineral densities. The liquid density was calculated by the method of Bottinga and Weill

Table 2. Experimental run data

Run No.	P (kbars)	T °C	Time (hours)	Capsule	Phases present	100 Mg/Mg + Fe charge	ol	opx
					Pyrolite - 40% olivine			
T-168	10	1300	0.17	Fe	ol + opx + quench cpx + gl	84.5	89.1	89.8
1012	10	1300	1	Pt	ol + opx + quench cpx + gl	86.2	89.1	89.9
T-89	10	1300	2	Pt	ol + opx + Cr + quench cpx + gl	86.9	91.0	89.8
T-144	10	1300	4	Pt	"	87.2	91.3	90.4
T-178	10	1300	7.5	Pt	ol + opx + cpx + Cr + quench cpx + gl	88.4	93.0	90.5
T-118	10	1350	2	Pt	ol + opx + Cr + quench cpx + gl	87.0	92.8	91.3
T-139	10	1350	0.5	Fe	ol + opx + quench cpx + gl	85.1	90.1	91.0
T-101	10	1450	2	Pt	ol + Cr + quench px + gl	89.7	95.8	-
T-138	10	1450	0.25	Fe	ol + quench px + gl	83.3	91.6	-
T-148	15	1350	2.5	Pt	ol + opx + cpx + Cr + quench cpx + gl	87.7	92.2	89.8
T-142	15	1400	1	Pt	ol + opx + Cr + quench cpx + gl	86.2	92.0	90.5
					Tinaquillo Lherzolite - 40% olivine			
T-155	10	1450	0.5	Pt	ol + Cr + quench px + gl	90.7	95.6	-

ol = olivine; opx = orthopyroxene; cpx = clinopyroxene; Cr = chrome spinel; gl = glass

(1970) using the least modified, most magnesian glass composition (obtained by reduced area rapid scans) with adjustment for the effect of pressure on the density (Kushiro *et al.*, 1976). Iteration of the mass-balance calculations to overcome the density difference between the equilibrium liquid and the analyzed glass made negligible difference to the resultant liquid composition. Two examples of liquids determined in this way are shown in Table 3, Figures 2 and 3, and Table 4, Figure 4. The SEM photographs of these runs are illustrated in Figure 1.

Point counting of phases was not possible for the high-degree melting runs where olivine alone or olivine and chrome spinel were residual phases, because of strong crystal settling within the charge even in runs of short duration. For these experiments (*e.g.* Fig. 5, Table 5) the liquid composition was calculated assuming a $K_D$ol/liquid of 0.3 (Roeder and Emslie, 1970; Green and Ringwood, 1967) after allowance for iron loss from the charge (Green, 1973).

Experimental results

In the three examples presented in detail in Figures 1–5 and Tables 1–5, the calculated equilibrium

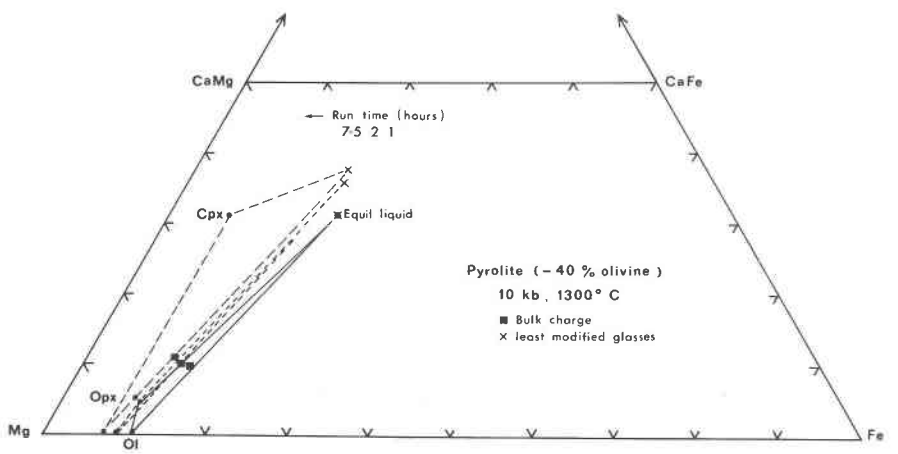

Fig. 3. Data from Fig. 2 for 1-, 2-, and 7½-hour runs at 10 kbar, 1300°C, illustrating effect of Fe loss. Squares indicate the bulk charge composition after the run. Tie lines join coexisting residual phases with least modified glass compositions. Note that the iron loss from the charge for the 7½-hour run has been sufficient to stabilize clinopyroxene in the residue.

Table 3. Compositions of phase for melting of pyrolite – 40 percent olivine at 10 kbar, 1300°C

	0.17 hours			1 hour					
	ol	opx	gl	large olivine[1] core	large olivine[1] rim[3]	small ol[2]	large opx core	large opx rim	melt[4]
SiO_2	40.5	54.8	52.0	40.6	40.5	41.0	55.1	54.0	49.8
TiO_2	-	0.47	2.87	-	-	-	0.43	0.85	2.7
Al_2O_3	-	2.93	13.2	-	-	-	2.52	3.63	12.5
FeO^t	10.5	6.39	8.99	10.5	10.3	10.2	6.42	6.24	9.0
MnO	-	-	-	0.20	0.34	0.40	-	-	0.1
MgO	48.3	31.7	9.11	98.1	48.5	48.0	31.7	31.1	12.0
CaO	0.31	2.35	11.0	0.39	0.36	0.38	2.42	2.58	10.9
Na_2O	-	-	1.97	-	-	-	-	-	2.4
K_2O	-	-	0.47	-	-	-	-	-	0.55
Cr_2O_3	0.38	1.30	0.35	-	-	-	1.35	1.60	-
Si	0.997	1.909		1.001	.996	1.007	1.921	1.885	
Ti	-	0.012		-	-	-	0.011	0.022	
Al	-	0.120		-	-	-	0.104	0.149	
Fe	0.216	0.186		0.216	0.211	0.209	0.187	0.182	
Mn	-	-		0.004	0.008	0.008	-	-	
Mg	1.771	1.649		1.767	1.780	1.758	1.647	1.618	
Ca	0.008	0.088		0.010	0.010	0.010	0.090	0.096	
Na	-	-		-	-	-	-	-	
Cr	0.007	0.036		-	-	-	0.037	0.044	
Total	3.000	4.000		2.999	3.005	2.993	3.997	3.996	
$\frac{100\ Mg}{Mg+Fe}$	89.1	89.8	64.3	89.1	89.4	89.4	89.8	89.9	70.4
Ca		4.6	33.1				4.7	5.1	
Mg		85.8	45.9				85.6	85.3	
Fe		9.7	21.0				9.7	9.6	

t = total iron as FeO

1. large olivine = $\geq 10\mu$

2. small olivine = $\leq 5\mu$

3. = rim compositions were obtained avoiding quench rims of pyroxene and olivine.

4. = calculated equilibrium melt composition, using modal analysis, analysed crystalline phase from 1-hr run and original bulk composition

liquid composition differs from the analyzed glass compositions. The nature of the calculated equilibrium melt at 10 kbar, 1300°C, produced by approximately 25 percent melting of pyrolite, is olivine tholeiite with 16 percent normative olivine; all analyzed glasses are higher in SiO_2 and lower in normative olivine than the calculated melts, with both the 0.17-hour and 7.5-hour runs containing normative quartz. At 15 kbar, 1350°C the degree of melting of pyrolite is about 18 percent and the equilibrium melt is alkali olivine basalt. All glass analyses are hypersthene normative and have considerably less MgO and more SiO_2, Al_2O_3, and CaO than the calculated melt. At 10 kbar, 1450°C the Tinaquillo lherzolite composition is about 40 percent molten, and the composition of the calculated melt, with very high MgO and SiO_2, is strongly hypersthene- and olivine-normative, resembling pyroxene-rich komatiitic liquids. In the follow-

Table 3. (continued)

2 hours						7.5 hours						
large olivine core	rim	small ol	large opx core	rim	gl	large ol core	rim	small ol	large opx core	rim	cpx	gl
40.7	41.0	40.8	54.8	55.0	51.3	41.2	41.0	41.0	55.0	55.3	53.1	51.2
-	-	-	0.42	0.42	2.85	-	-	-	0.52	0.50	0.70	3.12
-	-	-	2.72	2.40	12.4	-	-	-	2.70	2.66	3.33	13.2
8.70	8.30	8.21	6.42	6.23	8.93	7.57	6.96	6.90	5.97	5.72	4.59	7.64
0.35	0.35	0.36	-	-	-	0.21	-	-	-	-	-	-
49.8	49.80	50.2	31.7	32.4	10.4	50.7	51.7	51.8	31.9	31.5	21.7	10.2
0.41	0.60	0.39	2.45	2.50	11.8	0.36	0.32	0.40	2.70	3.22	15.0	12.1
-	-	-	-	-	1.86	-	-	-	-	-	-	1.90
-	-	-	-	-	0.50	-	-	-	-	-	-	0.58
-	-	-	1.46	1.05	-	-	-	-	1.20	1.08	1.53	-
0.995	0.999	0.995	1.912	1.915		1.000	0.993	0.992	1.913	1.923	1.906	
-	-	-	0.011	0.011		-	-	-	0.014	0.013	0.019	
-	-	-	0.112	0.099		-	-	-	0.111	0.109	0.141	
0.178	0.170	0.167	0.187	0.181		0.154	0.141	0.140	0.174	0.167	0.138	
0.007	0.007	0.008	-	-		0.004	-	-	-	-	-	
1.814	1.810	1.825	1.648	1.682		1.833	1.865	1.867	1.657	1.633	1.161	
0.011	0.016	0.010	0.092	0.093		0.009	0.008	0.010	0.101	0.120	0.576	
-	-	-	-	-		-	-	-	-	-	-	
-	-	-	0.040	0.029		-	-	-	0.033	0.030	0.044	
3.005	3.001	3.005	4.001	4.010		3.000	3.007	3.008	4.001	3.995	3.983	
91.1	91.4	91.6	89.8	90.3	67.5	92.3	93.0	93.0	90.5	90.8	89.4	70.3
			4.8	4.8	35.5				5.2	6.3	30.7	37.6
			85.5	86.0	43.5				85.8	85.1	61.9	43.9
			9.7	9.3	21.0				9.0	8.7	7.4	18.5

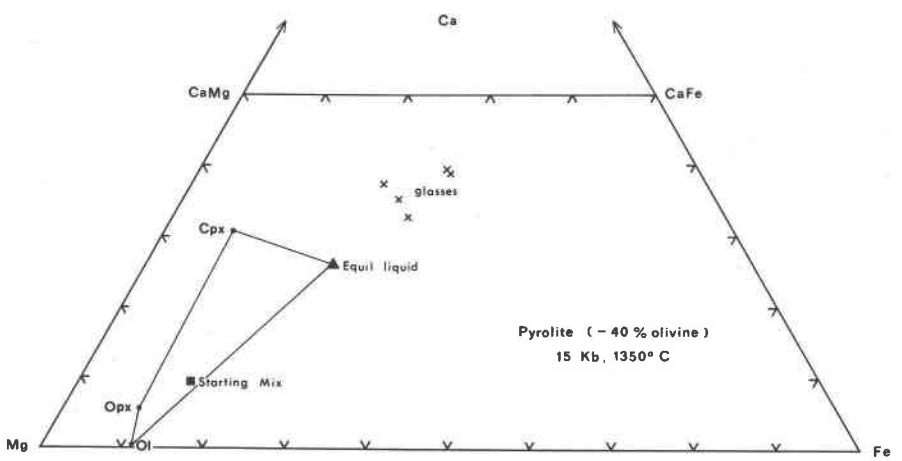

Fig. 4. Ca–Mg–Fe diagram illustrating the effect of quench growth of Ca pyroxene on the determined liquid compositions. The equilibrium liquid is calculated (see text). Compositions given in Table 4.

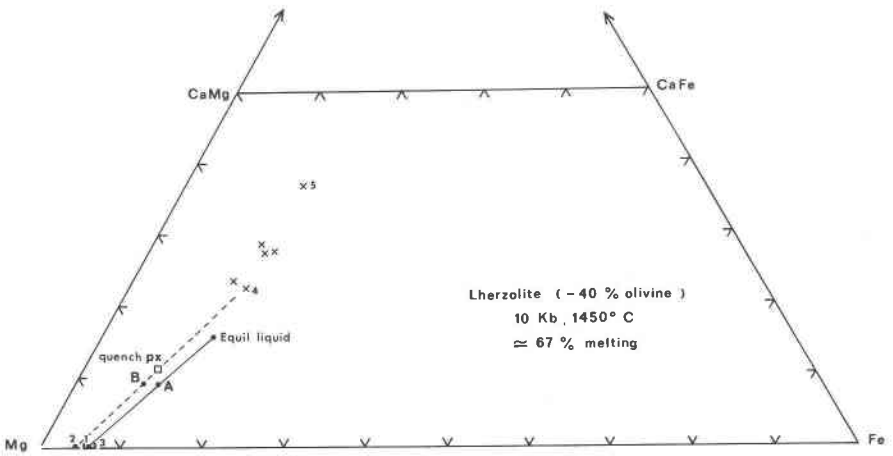

Fig. 5. Ca–Mg–Fe diagram illustrating relations in a run with a large amount of partial melting. Solid tie lines connect the starting mix (A) to the calculated equilibrium liquid. Dashed tie line joins analyzed olivine (2) with the bulk charge after the run (B) and the least-modified glass composition (4). Crosses indicate other glass analyses (determined at least 5–10 microns from any observable quench phase). Glass 5 was obtained adjacent (2–5μ) to a quench pyroxene. 3 = range of quench olivine compositions. Compositions given in Table 5.

ing sections we discuss the causes of these problems in determination of liquid compositions in partial melting experiments on peridotite compositions.

Iron loss in experimental runs

Although Stern and Wyllie (1975) showed in an andesite melting study that iron is not lost uniformly from the charge, there appears to be a belief that equilibrium, once achieved, is maintained throughout the experiment in spite of iron loss. For example, Mysen and Kushiro (1977) claim that a 20 percent iron loss results in only a minor change in the Fe content of the olivine and disregard any greater effect on the liquid composition.

Other data obtained from runs of varying duration at the same pressure and temperature, 10 kbar and 1300°C, are presented in Table 3 to illustrate the problem. Despite attempts to presaturate the Pt capsules, all experienced iron loss [shown by the 100Mg/(Mg+Fe) ratio of the charge; Table 2]; runs in spec-pure iron resulted in iron gain. The effect of iron loss can be very significant; for example, in the 7.5-hour run the iron loss was sufficient to stabilize calcic pyroxene in the residue, whereas only olivine, orthopyroxene, and chrome spinel were present in the residue of other runs. Figure 2 and the data of Table 3 show that as iron is lost from the system, demonstrated by increasing 100Mg/(Mg+Fe) ratio of the bulk charge, orthopyroxene compositions change little, whereas olivine and glass compositions readjust more rapidly to the loss. The different rates of adjustment of the crystalline phases to iron loss are also shown by the greater compositional difference between core and rim compositions of pyroxene relative to olivine. Stern and Wyllie (1975) found that apparent garnet and clinopyroxene Fe/Mg partitioning was dependent on run duration, because garnet adjusted more slowly to Fe loss than clinopyroxene, causing $(Fe/Mg)_{ga}/(Fe/Mg)_{cpx}$ to increase with run duration. Similar differences in the rate of adjustment of garnet and pyroxene to iron loss have been observed in eclogite melting studies (K. L. Harris, personal communication, 1978). The effect of iron loss from the system is shown in Figure 3, where all phases and the bulk composition are displaced from the equilibrium value to more Fe-poor compositions.

The effect of change of the bulk composition is most marked on liquid compositions: the 10-minute run in spec-pure Fe resulted in iron gain by both the charge and the glass, but had little effect on the compositions of residual crystals.

It is apparent that Fe diffusion rates are different for various phases and that iron is lost preferentially in the order liquid > olivine (orthosilicate) > pyroxene (chain silicate). Significant iron loss can result in the formation of olivine considerably more magnesian than the original equilibrium olivine because of attempted re-equilibration of the olivine with the increasingly iron-deficient liquid.

Equilibrium melting requires that equilibrium exists between melt and residue, and between residual phases. *However, the difference in rates of adjustment of the various phases to iron loss produces non-equilibrium assemblages.* Because of the different diffusion

Table 4. Compositions of phase and calculated melt for pyrolite – 40 percent olivine at 15 kbar, 1350°C

	ol[1]	opx	cpx	sp	glass[3]	melt[4]
SiO_2	41.1	54.7	52.4	-	49.9	49.0
TiO_2	-	0.33	0.80	1.23	3.4	3.2
Al_2O_3	-	3.93	5.03	25.3	14.4	12.9
FeO	7.53	6.25	5.09	21.7	8.7	10.2
MnO	0.41	-	-	-	-	0.1
MgO	50.6	30.8	20.5	16.3	8.3	11.6
CaO	0.35	2.76	14.3	0.27	10.9	9.1
Na_2O	-	-	0.55	-	3.3	3.1
K_2O	-	-	-	-	0.9	0.7
Cr_2O_3	-	1.15	1.42	35.2	-	-
$\frac{100\ Mg}{Mg + Fe}$	92.3	89.8	87.8	57	63	67
Ca		5.5	30.6		37.4	27.6
Mg		84.9	60.9		39.2	48.5
Fe		9.6	8.5		23.3	23.9

1. Equilibrium olivine used in liquid calculation was calculated assuming $K_D^{ol}/opx = 1.1$ i.e. 100 Mg/Mg+Fe = 88.9
2. Total iron as FeO
3. Least modified glass
4. Melt calculated by mass balance; using modal analysis, analyzed crystalline phases (olivine corrected for Fe loss) and original bulk composition

Table 5. Compositions of phases and calculated melt for lherzolite – 40 percent olivine at 10 kbar, 1450°C

	olivine	quench olivine	quench	spinel	glass[2]	melt[3]
SiO_2	41.6	44.5	50.9	-	54.8	51.6
TiO_2	-	0.12	0.32	0.13	0.4	0.2
Al_2O_3	-	1.34	6.46	11.5	8.9	7.8
FeO[1]	4.37	5.36	6.14	11.2	7.5	8.4
MnO	0.32	-	-	-	-	0.2
MgO	53.5	47.2	29.6	18.8	18.5	23.9
CaO	0.27	0.95	5.74	0.27	9.2	7.4
Na_2O	-	-	-	-	-	0.45
K_2O	-	-	-	-	-	0.04
Cr_2O_3	-	0.56	0.70	58.1	-	-
$\frac{100\ Mg}{Mg + Fe}$	95.6	94	89.6	74.9	81.4	83.8
Ca			11.1		22.6	15.7
Mg			79.7		63.0	70.5
Fe			9.3		14.4	13.9

1. Total iron as FeO
2. Least modified glass composition
3. Equilibrium melt calculated from K_D^{ol}/liq 1 0.3 after correction for iron loss (Green, 1973).

rates in liquid and different residual crystals, measured Fe/Mg partition coefficients are dependent on run time. For example, the $K_D$ol/opx = $(Fe/Mg)_{ol}/(Fe/Mg)_{opx}$ has been shown to be insensitive to temperature and pressure, and has been determined experimentally as equal to 1.1±0.1 (*e.g.* Mori and Green, 1978, and others). Equilibrated olivine–orthopyroxene pairs from natural peridotites have K_D values in this range (*e.g.* Nixon and Boyd, 1973; Himmelberg and Loney, 1973; Frey and Green, 1974), as do olivine–orthopyroxene pairs in experimental runs in capsule materials other than platinum-group metals (*e.g.* Kushiro *et al.*, 1972). Our data in Tables 2 and 3 commonly exhibit non-equilibrium Fe/Mg partitioning between olivine and orthopyroxene. This is also evident in some previous partial melting studies where iron loss has occurred; for example, the data of Mysen and Kushiro (1977) show $K_D$ol/opx ranging from 0.72 to 0.85, and these values can be attributed to Fe loss and preferential readjustment of olivine to more magnesian compositions. The extent of iron loss from their experiments can also be gauged by the fact that in some of their runs the starting composition lies outside the field defined by the analyzed phases.

Several methods of alloying Pt capsules with iron have been suggested to reduce iron loss (*e.g.* Nicholls, 1974; Ford, 1978). In order to avoid net exchange of Fe, the activity of Fe in the capsule must exactly match that in the silicate charge, *i.e.* this must be determined for each bulk composition, *T*, *P*, and run duration. Moreover Fe-alloyed Pt becomes brittle, difficult to seal, and may result in capsule fracture during the experiment. Methods such as those proposed by Ford (1978) and Johannes and Bode (1978) may considerably reduce iron loss, but do not remove the necessity for the investigator to thoroughly evaluate the nature and extent of compositional interchange between sample and container.

Quench modification of equilibrium melts

Scanning electron microscope photographs (Fig. 1) reveal the presence of some quench material in all our experiments, even where none was discernible

optically. The extent of quench material varies from narrow (0.5–1 micron) rims of pyroxene or olivine on primary phases to broader (2–5 microns) blades of quench pyroxene both as rims and as discrete dendrites in the glass. The dominant quench phase in these anhydrous runs is clinopyroxene with varying Ca content. Quench clinopyroxene is not surprising, since this phase most closely approximates the liquid composition over most of the melting range. Quench clinopyroxene commonly contains 6 to 12 percent Al_2O_3 and 6 to 16 percent CaO and has a high TiO_2 content (2–3 percent). These features, together with the generally lower 100Mg/(Mg+Fe) ratio and skeletal or dendritic form, serve to distinguish quench pyroxene from stable primary calcic pyroxene. In addition, quench pyroxene analyses generally are not stoichiometric. In most cases the 100Mg/(Mg+Fe) ratios of the quench and primary phases are distinct, but in some experiments a continuum was found. Because abundant quench material drastically reduces the liquid volume and results in increased concentration of highly incompatible elements in the residual melt fraction, the presence of quench rims and crystals will cause errors in any method of estimation of degree of melting or melt composition based on analysis of the glass in experimental runs.

Quench crystallization has been shown to significantly modify equilibrium melt compositions in hydrous melting of peridotite (Green, 1973, 1976), and we have therefore examined the effect of quenching on liquids in anhydrous melting experiments. Data from two experiments, one at low to moderate degrees of melting (15 kbar, 1350°C) and the other at a high degree of melting (10 kbar, 1450°C), are presented in Tables 4 and 5 and plotted on Ca–Mg–Fe (atomic) diagrams (Figs. 4 and 5). Diffusion studies (*e.g.* Hofmann and Magaritz, 1977) have shown a high efficiency of diffusion over short distances (*e.g.* $D = 10^{-6}$ cm^2 at 1400°C), but the quenching rate in solid-media apparatus is such as to produce large compositional differences within the glass where quench phases and outgrowths occur. Moreover, the glass compositions bear little relationship to the composition of the equilibrium liquid calculated by mass balance from the proportions and compositions of the residual phases (Table 4, Fig. 4) or using published partition coefficients (Roeder and Emslie, 1970) after correction for iron loss for simple residues (Table 5, Fig. 5). Glass analyses made adjacent to quench crystals show a marked compositional difference to those obtained in larger "quench-free" pools. In neither case can these be considered as equilibrium melts.

The new data reaffirm earlier studies of the quenching problem (Green, 1973, 1976; Cawthorn *et al.*, 1973) and show that marked changes in the liquid composition may result in partial-melting experiments where quench phases occur, even in anhydrous melting. This problem is especially severe at low degrees of melting, and previous studies have shown that the problem increases at higher pressure and in the presence of volatiles (Green, 1973, 1976; Nicholls, 1974; Mysen and Kushiro, 1977).

Conclusions

We believe that the problems of iron loss and quench crystallization in anhydrous partial melting studies employing piston-cylinder apparatus are severe enough in most cases to preclude direct determination of the equilibrium melt composition. At high degrees of partial melting quench modification is far from trivial, and at low degrees of partial melting modification of the melt may be as severe under anhydrous as under hydrous conditions. In all cases, iron loss problems in anhydrous melting are greater than under hydrous melting conditions because of the higher melting temperatures. Therefore we are forced to conclude that most, perhaps all, previously published partial melt compositions obtained by direct analysis of quenched glasses from piston–cylinder runs are in error. At the very least, all such compositions should be regarded with suspicion.

We have attempted to show that, provided run times are not unduly long (this must be determined empirically by repeated experiments of varying duration), it is possible to calculate the equilibrium liquid composition by mass balance from the compositions of the residual phases which adjust more slowly to iron loss (and using known K_D's for those phases which do adjust rapidly), provided the modal proportions of the phases (including the percentage of melt + quench) can be determined. This is possible by point counting of reflected light and SEM photographs of the polished mount where all phases, including quench phases and overgrowths, can be discriminated. Replicates are generally required to overcome inhomogeneous distribution and crystal settling. However, no liquid determined by partial-melting experiments can be regarded as safely estab-

lished in the absence of reversal studies (*i.e.* crystallization of the liquid composition under the same experimental conditions).

Acknowledgments

We thank W. O. Hibberson and W. C. Doran for technical assistance and advice, and Dr. A. McKee and B. J. Griffin for instruction in the use of the SEM microprobe. Comments on the draft manuscript by K. L. Harris and D. J. Ellis and reviews by W. C. Luth, P. L. Roeder, and R. F. Fudali are gratefully acknowledged.

References

Bottinga, Y. and F. F. Weill (1970) Densities of liquid silicate systems calculated from partial molar volumes of oxide components. *Am. J. Sci., 269,* 169–182.

Cawthorn, R. G., C. E. Ford, G. M. Biggar, M. S. Bravo and D. B. Clarke (1973) Determination of the liquid composition in experimental samples: discrepancies between microprobe analyses and other methods. *Earth Planet. Sci. Lett., 21,* 1–5.

Ford, C. E. (1978) Platinum–iron alloy sample containers for melting experiments in iron-bearing rocks, minerals, and related systems. *Mineral. Mag., 42,* 271–275.

Frey, F. A. and D. H. Green (1974) The mineralogy, geochemistry and origin of lherzolite inclusions in Victorian basanites. *Geochim. Cosmochim. Acta, 38,* 1023–1059.

Green, D. H. (1963) Alumina content of enstatite in a Venezuelan high-temperature peridotite. *Geol. Soc. Am. Bull., 74,* 1397–1402.

——— (1973) Experimental melting studies on model upper mantle compositions at high pressure under both water-saturated and water-undersaturated conditions. *Earth Planet. Sci. Lett., 19,* 37–53.

——— (1976) Experimental testing of 'equilibrium' partial melting of peridotite under water-saturated, high pressure conditions. *Can. Mineral., 14,* 255–268.

——— and A. E. Ringwood (1967) The genesis of basaltic magmas. *Contrib. Mineral. Petrol., 15,* 103–190.

Himmelberg, G. R. and R. A. Loney (1973) Petrology of the Vulcan Peak alpine-type peridotite, southwest Oregon. *Geol. Soc. Am. Bull., 84,* 1585–1600.

Hofmann, A. W. and M. Magaritz (1977) Diffusion of Ca, Sr, Ba and Co in a basalt melt: implications for the geochemistry of the mantle. *J. Geophys. Res., 82,* 5432–5440.

Ito, K. and G. C. Kennedy (1967) Melting and phase relations in a natural peridotite to 40 kilobars. *Am. J. Sci., 265,* 519–538.

Johannes, W. and B. Bode (1978) Loss of iron to the Pt-container in melting experiments with basalts and a method to reduce it. *Contrib. Mineral. Petrol., 67,* 221–225.

Kushiro, I., N. Shimizu, Y. Nakamura and S. Akimoto (1972) Compositions of coexisting liquid and solid phases formed upon melting of natural garnet and spinel lherzolites at high pressures: a preliminary report. *Earth Planet. Sci. Lett., 14,* 19–25.

———, H. S. Yoder and B. O. Mysen (1976) Viscosities of basalt and andesite melts at high pressures. *J. Geophys. Res., 81,* 6351–6356.

Mori, T. and D. H. Green (1978) Laboratory duplication of phase equilibria observed in natural garnet lherzolites. *J. Geol., 86,* 83–97.

Mysen, B. O. and A. L. Boettcher (1975) Melting of a hydrous mantle. II. Geochemistry of crystals and liquids formed by anatexis of mantle peridotite at high pressures and temperatures as a function of controlled activities of water, hydrogen and carbon dioxide. *J. Petrol., 16,* 549–593.

———and I. Kushiro (1977) Compositional variations of coexisting phases with degree of melting of peridotite in the upper mantle. *Am. Mineral., 62,* 843–865.

———, ———, I. A. Nicholls and A. E. Ringwood (1974) A possible mantle origin for andesitic magmas: discussion of a paper by Nicholls and Ringwood. *Earth Planet. Sci. Lett., 21,* 221–229.

Nehru, C. E. and P. J. Wyllie (1975) Compositions of glasses from St Pauls peridotite partially melted at 20 kb. *J. Geol., 83,* 455–471.

Nicholls, I. A. (1974) Liquids in equilibrium with peridotitic mineral assemblages at high water pressures. *Contrib. Mineral. Petrol., 45,* 289–316.

Nixon, P. H. and F. R. Boyd (1973) Petrogenesis of the granular and sheared ultrabasic nodule suite in kimberlites. In P. H. Nixon, Ed., *Lesotho Kimberlites,* p. 48–56. Lesotho National Development Corporation, Maseru.

O'Hara, M. J. and D. J. Humphreys (1977) Problems of iron gain and loss during experimentation on natural rocks: the experimental crystallization of five lunar basalts at low pressure. *Phil. Trans. R. Soc. Lond., A286,* 313–330.

Reed, S. J. B. and N. G. Ware (1973) Quantitative electron microprobe analysis using a lithium-drifted silicon detector. *X-ray Spectrometry, 2,* 69–74.

——— and ——— (1975) Quantitative electron microprobe analysis of silicates using energy dispersive X-ray spectrometry. *J. Petrol., 16,* 499–519.

Ringwood, A. E. (1966) The composition and origin of the earth. In P. M. Hurley, Ed., *Advances in Earth Science,* p. 287–356. MIT Press, Cambridge, Massachusetts.

Roeder, P. L. and R. F. Emslie (1970) Olivine–liquid equilibrium. *Contrib. Mineral. Petrol., 29,* 275–289.

Stern, C. R. and P. J. Wyllie (1975) Effect of iron absorption by noble-metal capsules on phase boundaries in rock melting experiments at 30 kb. *Am. Mineral., 60,* 681–689.

Manuscript received, August 21, 1978;
accepted for publication, May 16, 1979.